



28th International Conference on Knowledge-Based and Intelligent Information & Engineering Systems (KES 2024)

## Simulation-based dataset acquisition for robotic cardiac ultrasound examinations

Shuping Kang<sup>a\*</sup>, Thomas Daniels<sup>a</sup>, Rossitza Setchi<sup>a</sup>, Yulia Hicks<sup>a</sup>

<sup>a</sup> *Research Centre in AI, Robotics and Human-Machine Systems (IROHMS), Cardiff University, Cardiff CF24 3AA, UK*

---

### Abstract

Over the past decade, automating ultrasound scanning has been the subject of intense research. However, training a robot to perform automated ultrasound examinations requires a substantial corpus of training data. Traditionally, researchers have sought to obtain such data either through publicly available datasets or by engaging professional sonographers in experiments aimed at dataset generation. The former approach often yields incomplete datasets insufficient for specialized research objectives, while the latter entails logistical challenges, including the necessity for frequent manual experimentation and ready access to medical professionals. Therefore, the acquisition of a comprehensive and suitable dataset remains an essential yet formidable challenge. Here, we propose a novel framework for achieving the automated acquisition of cardiac ultrasound datasets by controlling robot behaviour using a digital twin within a simulated environment. This framework consists of two modules: physical and virtual. Within the virtual simulation module, diverse body models of varying dimensions can be inputted, enabling the planning of robot arm path and ultrasound scanning manoeuvres. Then the physical robot arm clones the actions of the robot in the simulation environment and updates its current state in the virtual module. The proposed framework was used to collect 43,000 cardiac ultrasound images from 8 patients with different pathologies and 1 healthy individual using a KUKA LBR Med robot and Intelligent Ultrasound Simulator. It is also expected to be feasible for a real-person dataset collection.

© 2024 The Authors. Published by Elsevier B.V.

This is an open access article under the CC BY-NC-ND license (<https://creativecommons.org/licenses/by-nc-nd/4.0>)

Peer-review under responsibility of the scientific committee of the 28th International Conference on Knowledge Based and Intelligent information and Engineering Systems

*Keywords:* cardiac; ultrasound; dataset collection; simulations; robot; digital twin.

---

\* Corresponding author.

*E-mail address:* KangS9@cardiff.ac.uk

## 1. Introduction

Ultrasound scanning has become one of the most reliable and widely used diagnostic methods for various diseases because of its outstanding advantages compared to other imaging modalities including non-invasiveness, lack of ionising radiation, affordability, and real-time capability [1]. However, despite the rapid technological developments in recent years, clinical ultrasound diagnosis is not widely used in primary care. For example, due to the inconsistency and varying operation techniques between different clinicians, the quality of the scanning image obtained is highly dependent on the expertise of the sonographers, leading to potential misdiagnosis [2]. During a typical ultrasound exam, sonographers perform frequent and various physically demanding movements of the shoulders, back, neck, wrist, and so on [3]. Coupled with exposure to heavy workload, many sonographers suffer from musculoskeletal disorders [4]. For example, 84% of the sonographers interviewed during a study revealed frequent or permanent suffering from pain [5]. Therefore, appropriate solutions to address these issues are urgently needed, which is why ultrasound robotics has garnered widespread attention.

Robotic ultrasound examination is a medical imaging modality that utilizes a robotic arm equipped with an ultrasound transducer to perform scans on a patient. Compared with human doctors, the performance of a robotic system is more accurate, flexible, repeatable, fatigueless, and robust [6]. It can also release the sonographers from their heavy workload. Nevertheless, training a robotic system capable of autonomously recognizing ultrasound views and making actionable decisions based on these views is very challenging. One indispensable aspect is the requirement for a large quantity of high-quality training data, particularly for complex human organs such as the heart. The structure of the heart is inherently more complex than that of other organs. Additionally, during examinations, consideration must be given to the shadowing caused by rib obstruction, as the heart is not a superficial organ. Furthermore, the continuous motion of the heart also exacerbates the difficulty of machine recognition. All these issues collectively render machine recognition exceptionally challenging. Currently, manually acquired datasets pose considerable usability barriers owing to their limited information over acquisition conditions. This is particularly concerning certain complex structures of human tissues, for which online data often prove insufficiently comprehensive. For example, most publicly available cardiac ultrasound image datasets consist primarily of images and labels [7], [8]. These datasets are extensively utilized for classification of various standard views, yet there is a notable scarcity of datasets containing information, which is needed to train a robot perform an ultrasound examination such as the pose status of the probe and the corresponding contact force with the skin.

To the best of our knowledge, there currently exists no cardiac ultrasound dataset acquired through robotic automation. The objectives of this study are twofold. Firstly, to design a robotic system capable of autonomously acquiring a dataset of cardiac ultrasound images. Secondly, to obtain a set of experimental data suitable for machine learning training. Within cardiac ultrasound examinations, several commonly utilized scanning windows exist, with the Parasternal long axis (PLAX) view being a crucial standard view within the Parasternal window. Primarily utilized for assessing cardiac cavity enlargement, valve dynamics, and myocardial condition, the PLAX view facilitates the diagnosis of conditions such as myocardial infarction, cardiomyopathy, valvular disease, and arrhythmia [9]. The full dataset would comprise PLAX views along with corresponding probe positions, rotation angles, tilt angles, and contact forces. As the probe scans through the region of interest, the dataset will include ultrasound views with varying quality, which can be used in future in the subsequent training of agents capable of either replacing or assisting sonographers in cardiac ultrasound examinations.

## 2. Literature review

Ultrasound (US) is a noninvasive imaging modality which employs high-intensity sound waves to delineate internal anatomical structures, thereby helping clinicians in diagnosing a spectrum of medical pathologies. Variations in tissue composition result in differential reflection of sound waves, which are subsequently processed by a computer to ascertain the position, shape, and structure of the organs. The resultant data is visualized as US images on the accompanying monitor [10]. Various databases have been collected and utilized for training a robot system capable of performing US examinations automatically or for developing algorithms capable of recognizing and classifying standard US views, among other purposes. The prevailing publicly available US image datasets, such as those referenced in [11] and [12], typically lack information regarding the spatial orientation of the US probe (US

transducer) during their acquisition process. For example, the dataset created by Soemantoro et al. [13] trained a window search algorithm to control the motion of an US probe to locate the two standard acoustic windows of the heart. To satisfy the data requirements of this algorithm, the authors obtained three databases from various sources, all acquired manually. These databases originated from Milton Keynes University Hospital using a medical cardiac US system (Philips Epiq CVX), the HeartWorks US simulator, and a portable GE Vscan Extend US device for a healthy participant.

These datasets are extensive and diverse but lack spatial tracking, thereby impeding their utility in image-guided procedures reliant on spatial information. To address this limitation, the scientific community have released tracked US image datasets, such as [14] and [15].

The goal of the research presented in [14] was to train an intelligent agent to predict autonomously the next probe motion during kidney US examinations conducted on a human body. To achieve this, the doctors were asked to perform kidney US demonstrations on five volunteers, during which US images, along with their corresponding posture and contact force, were meticulously documented. This process resulted in the acquisition of a dataset comprising over five thousand data instances. This is valuable as the collected database incorporates both force and pose information.

Meanwhile, to advance US image registration and three-dimensional (3D) volume reconstruction algorithms, the dataset described in [15] was developed by manual scanning of the abdominal phantom using a tracked US probe integrated with an optical tracking system. This dataset [15] records the location of the US probe for each US image and includes US images obtained under varying acquisition parameters such as frequency, focal depth, gain, power, dynamic range, among others.

Another relevant dataset [16] comprises manually acquired US images and Magnetic Resonance Images (MRI) of brain tumours from 14 patients, specifically designed to facilitate the evaluation of US registration algorithms in comparison to MRI scans of the corresponding patients.

Another study which is uniquely focused on the automation of robotic US data acquisition [17], contains two datasets by programming the robot to traverse straight line path on a baby phantom and a square wave path on an amplitude phantom. These datasets include not only US images but also information regarding the probe pose and applied force corresponding to each image. The datasets are deemed reliable as they have been validated for three-dimensional model reconstruction. Furthermore, the authors conducted simulated robot motion, enhancing system safety measures. However, the medical phantoms utilized in this study only include models of individual organs or tissues, without considering their location within the human body. Therefore, the datasets obtained do not contain the spatial relationship between organs and the human body, and do not account for issues such as obstruction by other organs or anatomical structures during the scanning process.

While the datasets mentioned hold significance, manual acquisition of US image datasets entails inherent drawbacks, including the potential for arbitrary and imprecise control over the positioning and force exerted by the sensing device [17]. This variability in image quality consequently constrains the utility of such datasets within environments requiring image recognition or classification. In addition, there are very few studies on utilizing robots to obtain ultrasound data, and the existing related studies primarily focus on model scanning of simple tissues. This is because when a robot collects data from a real human body, it not only needs to consider the safety and comfort of the person being tested, but also the significant differences between individuals due to their complex anatomical structures. Furthermore, current existing datasets of cardiac US views notably lack comprehensive inclusion of both corresponding positional and force information of the probe. Therefore, it can be concluded that training a robot system capable of ensuring the smoothness and precision of the experimental process for automatic US dataset collection is essential. Similarly, it is necessary to acquire a cardiac US dataset containing spatial information.

### 3. Conceptual framework

This section explains the proposed framework in detail, as show in Fig. 1. Here, a method called “digital twin” is applied. A 3D graphics body model and a robotic model were constructed in the simulation software for algorithm editing and validation of robot motion. Then, simulation was utilized to synchronously control robot motion in the physical environment. This approach primarily reduces safety concerns regarding the examined human body and

robotic arm, affording the ability to safely visualize and test various scenarios in a controlled and accurate virtual environment before implementing them in the real world.

Within this framework, initially, we utilize a 3D camera to acquire a point cloud model of the body to be scanned, which is then imported into simulation software after simple processing. Subsequently, scanning path planning and robot motion programming are conducted within the simulation software. Following the connection of software with the robot and the calibration of the robot's position in the physical environment, data collection motion is executed by the robot in the physical environment under the control of the simulation environment, thereby acquiring the dataset. Throughout this process, all US data, including US images, probe position coordinates, orientations, contact forces, and tilt angles, are recorded. Furthermore, to ensure the safety of the US simulator, the contact force between the probe and the surface of the simulator is constrained within a specified range using the robot's built-in force sensor. This regulation is facilitated by the robot's internal force sensor, which is coupled with external MATLAB programs. The measured force is recorded and utilized as feedback in the simulation model to adapt the probe's motion accordingly. The robotic system integrates advanced digital twinning methods, leveraging robotic motion in virtual environments to guide its real-world actions. This approach facilitates the incorporation of varied human body models as scanning targets in simulated environments, thereby overcoming some constraints encountered in the physical world. Additionally, it enables pre-testing to mitigate safety concerns associated with scanning on human subjects, offering a potential new avenue for future acquisition of US experimental data.

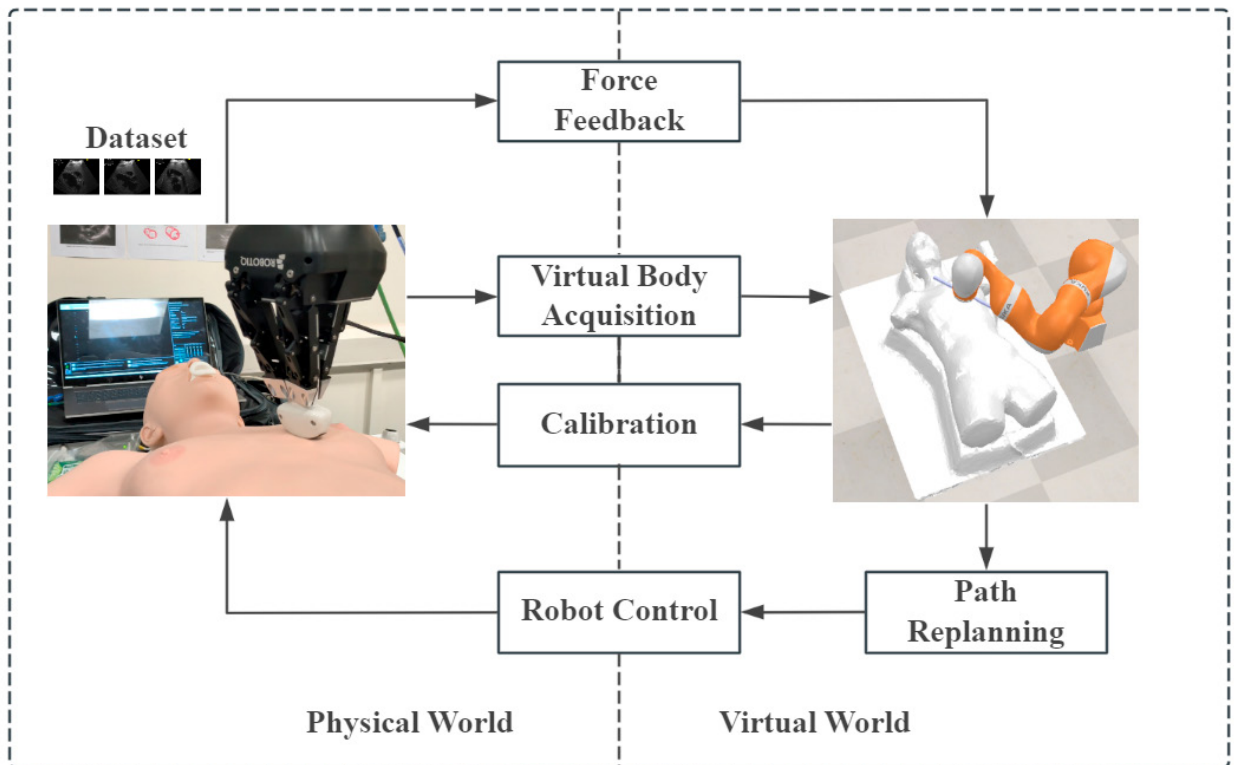


Fig. 1. Digital twin conceptual framework for automatic acquisition of ultrasound images

#### 4. Experimental setup

This section provides an overview of the laboratory's equipment used in this work, detailing the protocols utilized for cardiac US data acquisition. Additionally, it explores the robotic approach to US scanning and outlines the expected data types and structures targeted for acquisition.

#### 4.1. Equipment

This study uses a KUKA Light-Weight Robotic arm (LBR Med 14 R820, KUKA Deutschland GmbH, Augsburg, Germany) (Fig. 2(a)). It has 7 axes and is designed to fulfil precise medical specifications. Equipped with responsive sensors, meticulous safety measures, surfaces tailored for hygiene optimization, and a controller engineered for seamless human-robot collaboration, this robot is suitable for a diverse array of assistive systems within medical technology. Here, the robot is running in Cartesian impedance control mode.

In view of the safety concerns during the experimental process, we employed an intelligent hybrid software and hardware US simulator BODYWORKS|Eve, shown in Fig. 2(b). That is a high-fidelity, AI-powered US simulator designed for medical education and training. It is based on advanced physics-based modelling, which allows for realistic 3D simulations of the organs like heart, liver, kidney, and their surrounding structures.

To facilitate simulation by obtaining a mesh model of the human body and accurately positioning of the simulated human bodies and robots relative to each other, a depth camera with a certain level of precision is essential. Here, a RGB camera D455 shown in Fig. 2(c) from Realsense™, Intel® is chosen. The D455 camera offers heightened accuracy and adaptability across diverse utilization scenarios. The integration of an Inertial Measurement Unit (IMU) enables applications to enhance their depth perception under conditions involving camera movement. This augmentation facilitates enhanced environmental awareness, which is crucial for robotics.

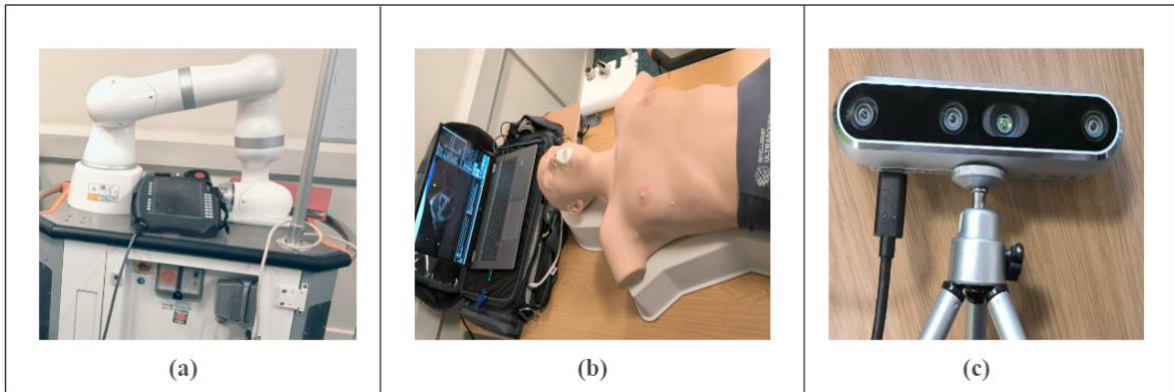


Fig. 2. Main equipment used in the study (a) KUKA Light-Weight robotic arm; (b) US simulation phantom; (c) RealSense camera.

#### 4.2. Calibration

To ensure the alignment of the robot and simulator positions in the real world with the simulation environment, calibration of the robot's position in the real world is required before experiment. During the initial calibration, the robot's position in the real world is adjusted by iteratively controlling its motion via digital twinning to reach the optimal starting scanning position, which is manually marked on the simulator. At this point, the end effector in the simulation environment has reached the optimal scanning point on the simulator, but there may still be some discrepancies in the real world. Therefore, minor adjustments to the simulator or robot position are made while maintaining the robot's posture until the marked starting point is reached. After the initial calibration, the positions of the robot, simulator, and end effector are marked and the coordinates of three reference points on the simulator are recorded.

#### 4.3. Experimental protocol

The human heart is located within the mediastinum, between the lungs under the sternum, specifically at the level of thoracic vertebrae T5-T8 [18]. The upper part of the heart is located at the level of the third costal cartilage. Its apex, or lowermost point, is situated to the left of the sternum and approximately 8 to 9 cm away from the midsternal

line, between the junction of the fourth and fifth ribs where they articulate with the costal cartilages [19]. In anatomical terms, this location is situated slightly leftward and inferiorly in relation to the left nipple in male patients, or laterally beneath the left breast in female patients. Considering the anatomical context of the subject under study, this region can be estimated to be situated approximately midway along the torso, toward the anatomical left side of the patient [13]. In the present work, we focus on the acquisition of a dataset necessary for the training of an automated system aimed at procuring the PLAX view of the heart in view of its important role in cardiac condition monitoring.

To achieve an optimal PLAX view, it is recommended to position the transducer slightly left of the sternum within the 4th or 5th intercostal space and rotate the transducer until the orientation of the marker on it directly towards the right shoulder. Also, alignment of the US beam parallel to an imaginary line drawn from the patient's right shoulder to their left hip is crucial [20]. The acquired images depict anatomical cross-sectional views along the long axis of the heart, with the apical segment positioned towards the left side of the screen and the base towards the right. In more detail, the right ventricular outflow tract (RVOT) is discernible at the uppermost region of the image, the inferolateral (or posterior) wall towards the bottom, the aorta towards the right, and the cardiac apex towards the left. And the anteroseptal region is delineated between the RVOT and the cavity of the left ventricle (LV) [21].

In the collected data, it is imperative to ensure the inclusion of high-quality PLAX views of the cardiac thoracic cavity. A good visualization (Fig. 3) occurs when both the aortic valve (AV) and mitral valves (MV) are distinctly visible and aligned slightly to the right of the centre on the display [20]. In an ideal PLAX view, notable features include the discernible presence of the anterior and posterior mitral valve leaflets (AML, PML), the aortic valve (AV), and the descending aorta (DA), alongside the absence of the LV apex and the near-horizontal alignment of the LV wall [22].

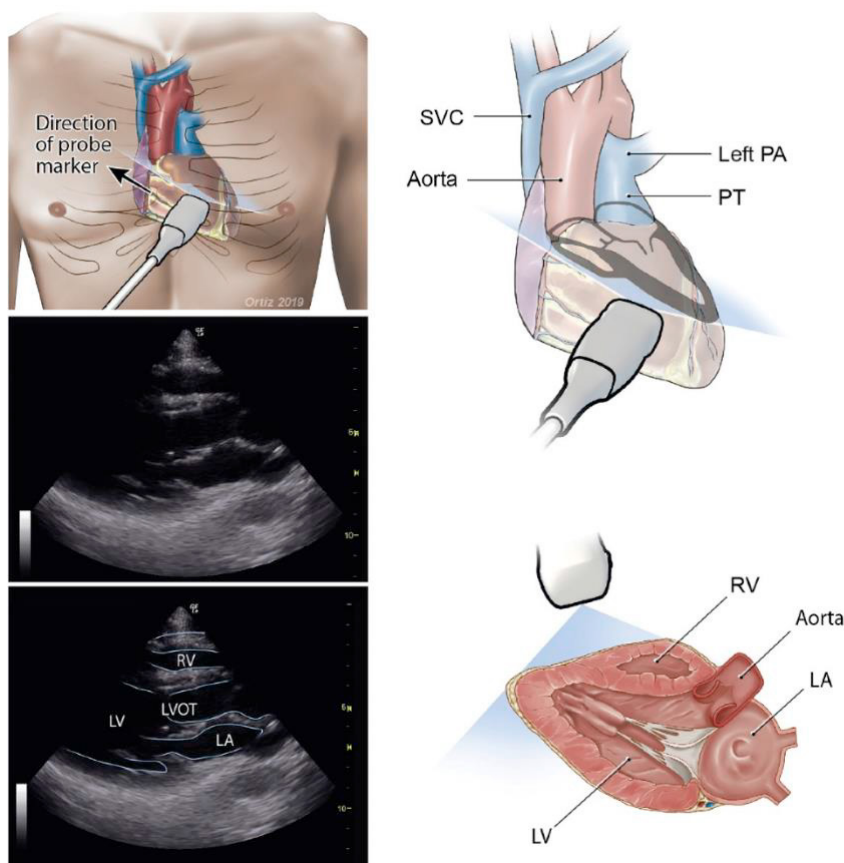


Fig. 3. Direction of probe, the US images, and the structure illustration of PLAX view of human's heart. Illustration by Angélica Ortiz ©2019, provided under CC-BY-NC-ND, while being reprinted with permission from [17].

#### 4.4. Data collection

Typically, the heart rate remains around 72 beats per minute at rest, nearly 0.83 second per beat, with exercise resulting in a transient increase that ultimately contributes to improved heart health and a lower resting heart rate [23]. With each cardiac cycle, the atria and ventricles undergo one contraction and one relaxation. The period of relaxation is called diastole while the period of contraction is called systole. Diastole is the longer of the two phases so that the heart can rest between contractions. Usually, systole lasts 0.3 to 0.4 second [24]. Therefore, to ensure that the acquired data encompasses various states of cardiac motion as comprehensively as possible, we designed the acquisition of data images at intervals of 0.2 to 0.3 seconds. In this context, US image acquisition is achieved through screen capture. As the corresponding position coordinates of the probe, the angle of rotation, and the tilt angle information are all fed back to the same webpage, the acquisition is performed via webpage data extraction. Contact force, on the other hand, is separately obtained through force sensing by the robot. Commands for both screen capture and webpage data extraction are scripted within the same python program. Due to the time required for program execution, there remains an approximate 0.15-second delay between screen capture and data extraction. Nevertheless, given the notably low velocity of probe movement during experimental US scanning, the impact of this time delay can be considered negligible. The dataset comprises data from eight distinct patients with varying pathological conditions and one healthy individual. These individuals exhibit differences in age, gender, and pathology including but not limited to conditions such as low left ventricular failure, mitral stenosis, pulmonary embolism, and mitral regurgitation. Additionally, the images within the dataset depict a spectrum of natural echocardiographic variations, reflecting patient-specific variables and imaging indications present in our comprehensive clinical database. These variations encompass differences in zoom, depth, focus, sector width, gain, systole/diastole. Overall, at a given position, with only variations in probe direction and tilt angle, a total of 43,000 data samples are acquired.

## 5. Experiments

### 5.1. Planning scanning trajectory.

According to the operational guidelines for acquiring the standard PLAX view of the heart, to locate a good-quality PLAX view, it is imperative to first identify the cardiac Parasternal window, which is the starting point here. Once the starting point is determined, the probe only needs to perform rotating, tilting, and rocking movements to locate the optimal long-axis view. Based on the assumption made in this study that subsequent training of the robotic system for automated US examinations does not consider the issue of finding the starting point, data collection for locating the starting point is not conducted here. Therefore, the starting point will be manually identified and marked before the experiment. For the robot, it first needs to obtain this marked starting point. and then the US probe is rotated to orient the marker on the probe towards the right shoulder (with the direction of the marker on the screen adjusted to the right side). Subsequently, adjustments are made to align the direction of the US beam as parallel as possible to an imaginary line drawn from the patient's right shoulder to left hip. Fine adjustments to the tilt angle and orientation of the probe are then made until a satisfactory US image is observed on the screen (Fig. 4). It is noted that the rotation angle of the probe from the initial direction, for most humans, as well as the medical phantom here, parallel to the central axis, is approximately 45 degrees, while the tilt angle is small. Therefore, the rotation range of the probe is set to 20 degrees, allowing for clockwise and counterclockwise rotations of ten degrees each in the standard direction for data collection. Furthermore, the tilt angle of the probe is limited to ten degrees. This approach aims to enhance the model's applicability across a broader spectrum. Additionally, given that the system's reliance on predefined parameters may not fully account for the variability in patient anatomy and physiology encountered during actual US examinations, future modifications could involve converting these data into user-editable formats. This would allow for adjustments based on individual anatomical proportions, enhancing the system's adaptability and precision in diverse clinical scenarios. The actions for scanning are described as follows:

- 1) First The robot reaches a position approximately 50 cm above the starting point, and subsequently approaches slowly until it contacts the simulated surface of the medical phantom.
- 2) Then, the US probe is rotated 55 degrees perpendicular to the horizontal plane, orienting the marker on the US probe towards the right shoulder of the body.



3) Subsequent to this step, while retaining the probe's position and orientation, a gradual tilting of the probe is executed, inducing a lateral inclination of 5 degrees to both directions.

4) Final step involves rotating the probe 1 degree clockwise along the direction that moves the marker on the probe above the centre of the phantom. This procedure is repeated 20 times on one patient to cover the range of 20 degrees.

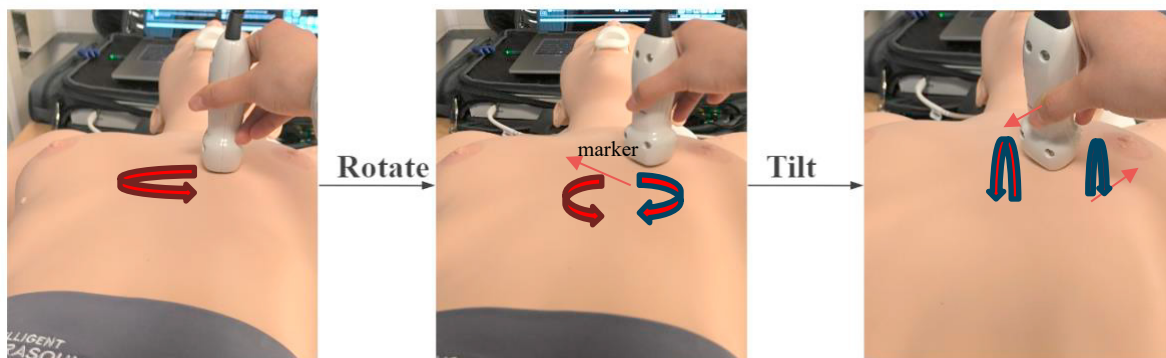


Fig. 4. The procedure of searching for a good PLAX view.

## 5.2. Motion control of the robot

To achieve probe positioning and force control during robot-assisted scanning, a hybrid position-force control was implemented. Within the force control task subspace of the robot, the probe maintains contact with the surface of the medical body model, with the contact force constrained to be within 12-18N. It is noteworthy that during actual US examinations on the human body, the magnitude of the contact force between the probe and the skin not only determines the comfort and safety of the examinee but also influences the final US imaging quality. However, as the imaging quality of our US simulator is not affected by the applied pressure, variations in pressure within this dataset are solely intended to ensure comfort and safety. Within the position control task subspace, the motion position of the end effector is controlled through robot Inverse Kinematics to enable probe traversal across the scanning area. To ensure smooth and safe motion, the robot is constrained by maximum velocity and acceleration limits, ensuring that its motion within each segment is slow and uniform. Upon commencement of the robotic arm's motion, the end-effector initially approaches medical phantom to be scanned from the starting position. During this (first) phase, the speed is maintained at a constant rate, which is relatively higher compared to later stages. The same speed is kept until the probe reaches a point directly above the scan target, approximately 50cm above. Subsequently, in the second stage, the speed is reduced to a small value as it approaches the surface of the object to be scanned until the probe makes contact and maintains a limited pressure. The speed is then further reduced for rotation to the scanning orientation to conduct US scanning and collect data in the last stage. Throughout this process, the robot remains continuously in motion, only decelerating at specific positions. Generally, it takes an expert between 15 and 60 minutes to perform a Transthoracic echocardiogram (TTE) examination on a patient in the hospital. Here, to ensure that the collected data encompasses various heart movement conditions and perspectives as comprehensively as possible, the robot moves very slowly. Consequently, the experiment on each patient takes approximately 16 minutes. The robotic system operates in impedance control mode, facilitating the regulation of dynamic interactions with its surrounding environment. This utilization of impedance control prioritizes the system's responses to collisions. Through the adjustment of stiffness and damping parameters, the system's reactions can be customized to suit specific applications, thereby augmenting overall safety throughout the operational process. Fig. 5 shows some pictures from the test using impedance control mode in conjunction with a digital twin simulation.



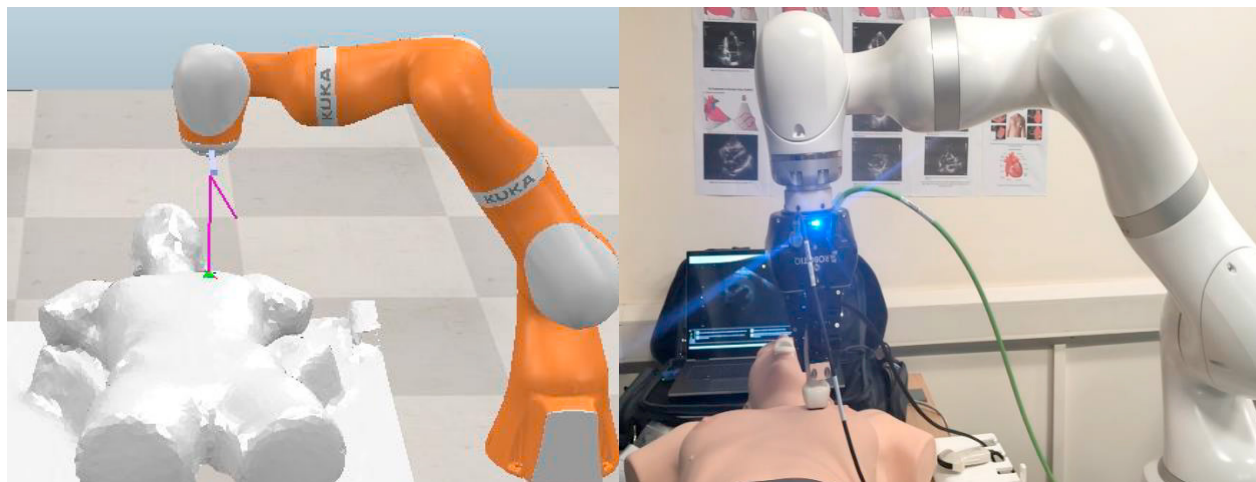


Fig. 5. Motion planning test based on Digital Twin

### 5.3. Obtained data

The dataset consists of 43,000 samples of data, each sample denoted as  $\{I_i, F_i, P_i, R_i, T_i\}$  where  $i$  denotes the numerical naming convention for images.  $I_i$  denotes the US image called  $i$ ,  $F_i$  denotes the contact force corresponding to the acquisition of the NO.  $i$  image,  $P_i$  signifies the coordinates of the probe during the acquisition of the NO.  $i$  image,  $R_i$  indicates the orientation of the probe during the acquisition of the NO.  $i$  image, and  $T_i$  represents the tilt angle of the probe during the acquisition of the NO.  $i$  image. Fig. 6. presents three examples of the obtained images, among which the first two are better PLAX views, since both the AV and MV are better visible.

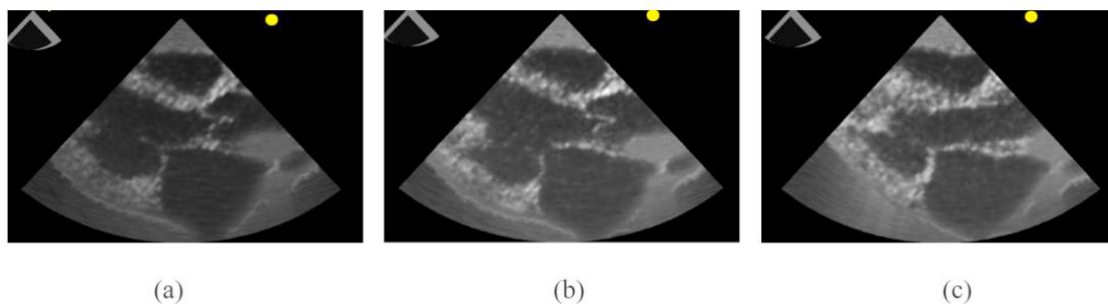


Fig. 6. Several images collected from medical phantom.

## 6. Conclusions and future work

This paper describes a robotic system designed for the automated acquisition of datasets required for training US examination algorithms. The robot is controlled by employing digital twinning and inverse kinematics. Force sensors and torque sensors are used to obtain contact force feedback. Image and positional information of probe are collected using an automated screen capturing algorithm and a web scraping algorithm. Theoretically, with the positioning function of KUKA robot, this system could be adapted for human US scanning data collection. Furthermore, the paper presents a dataset aimed at training robots to autonomously locate optimal cardiac PLAX views. This dataset comprises both the US images as well as the positional coordinates, orientation, tilt angles, and contact force corresponding to each image. This work is the first step towards developing training algorithms to acquire standard US views. In the future, we hope to validate the performance of the system on real humans and finally expand the

scope of this system to encompass real human data acquisition, with the aspiration that this dataset will contribute to training robots for autonomous US examinations. It is expected that more experiments on people with different physical conditions such as genders, pathologies, height will be conducted. Potential challenges in the clinical field such as addressing the imaging effects caused by respiratory motion as well as ensuring the safety and comfort of patients during the examination process will be also considered.

## Acknowledgements

The authors would like to acknowledge James Stratford for his help on the three-dimensional models of medical phantom and Intelligent US company for providing positional and postural feedback for the US probe of the phantom.

## References

- [1] Keyu. Li, Yangxin. Xu, and Meng. Q.-H. Meng. (2021), “An Overview of Systems and Techniques for Autonomous Robotic Ultrasound.” *IEEE Transactions on Medical Robotics and Bionics*, **3**(2): 510–524.
- [2] Alexander. Rykkje, Jonathan. Frederik. Carlsen, and Michael. Bachmann. Nielsen. (2019), “Hand-Held Ultrasound Devices Compared with High-End Ultrasound Systems: A Systematic Review.” *Diagnostics*, **9**(2): Art. no. 2.
- [3] Gill. Harrison and Allison. Harris. (2015), “Work-related musculoskeletal disorders in ultrasound: Can you reduce risk?” *Ultrasound*, **23**(4): 224–230.
- [4] Grahame. Brown. (2003), “Work Related Musculoskeletal Disorders in Sonographers.” *BMUS Bulletin*, **11**(3): 6–13.
- [5] Tamader. Y. AL-Rammah, Areej. S. Aloufi, Saffana. K. Algaed, and Noura. S. Alogail. (2017), “The prevalence of work-related musculoskeletal disorders among sonographers.” *Work*, **57**(2): 211–219.
- [6] Daniel. R. Swerdlow, Kevin. Cleary, Emmanuel. Wilson, Bamshad. Azizi-Koutenaeei, and Reza. Monfaredi. (2017), “Robotic Arm-Assisted Sonography: Review of Technical Developments and Potential Clinical Applications.” *American Journal of Roentgenology*, **208**(4): 733–738.
- [7] Zhe. Huang, Gary. Long, Benjamin. Wessler, Michael C. Hughes. (2021), “A New Semi-Supervised Learning Benchmark for Classifying View and Diagnosing Aortic Stenosis from Echocardiograms.” Proceedings of the 6th Machine Learning for Healthcare Conference.
- [8] David. Ouyang<sup>1</sup>, Bryan. He, Amirata. Ghorbani, Neal. Yuan, Joseph. Ebinger, Curtis P. Langlotz<sup>1</sup>, Paul A. Heidenreich<sup>1</sup>, Robert A. Harrington<sup>1</sup>, David H. Liang, Euan A. Ashley and James Y. Zou. (2020), “Video-based AI for beat-to-beat assessment of cardiac function.” *Nature*, **580**(7802): 252–256.
- [9] Shida. Yuuki, Kumagai. Souto, Tsumura. Ryosuke and Iwata, Hiroyasu. (2023), “Automated Image Acquisition of Parasternal Long-Axis View with Robotic Echocardiography.” *IEEE Robotics and Automation Letters* 8, 5228–5235.
- [10] InformedHealth.org. (2020), “In brief: How do ultrasound examinations work?” Cologne, Germany: Institute for Quality and Efficiency in Health Care (IQWiG). [Online]. Available: <https://www.ncbi.nlm.nih.gov/books/NBK563109/>
- [11] S. Balocco et al., (2014), “Standardized evaluation methodology and reference database for evaluating IVUS image segmentation.” *Computerized Medical Imaging and Graphics*, **38**(2): 70–90.
- [12] Jia-wei. Tian, Ying. Wang, Jian-hua. Huang, Chun-ping. Ning, Han-mei. Wang, Yan. Liu, Xiang-long. Tang. (2008), “The Digital Database for Breast Ultrasound Image.” in 11th Joint International Conference on Information Sciences, Atlantis Press, pp. 414–418.
- [13] Raska. Soemantoro, Attila. Kardos, Gilbert. Tang, and Yifan. Zhao. (2023), “An AI-powered navigation framework to achieve an automated acquisition of cardiac ultrasound images.” *Sci Rep*, **13**(1): Art. no. 1.
- [14] Yiwen. Chen, Chenguang. Yang, Miao. Li, and Shi-Lu. Dai. (2021), “Learning to Predict Action Based on B-ultrasound Image Information.” in *2021 6th IEEE International Conference on Advanced Robotics and Mechatronics (ICARM)*, pp. 492–497.
- [15] Vikas. Revanna. Shivaprabhu, Andinet. Enquobahrie, Zach. Mullen, and Stephen. Aylward. (2013), “Accelerating ultrasound image analysis research through publicly available database.” in *Medical Imaging 2013: Ultrasonic Imaging, Tomography, and Therapy*, SPIE, pp. 319–325.
- [16] Laurence. Mercier, Rolando. F. Del Maestro, Kevin. Petrecca, David. Araujo, Claire. Haegelen, and D. Louis. Collins. (2012), “Online database of clinical MR and ultrasound images of brain tumors.” *Medical Physics*, **39**(6): Part1, pp. 3253–3261.
- [17] Camilo. Cortes, Luis. Kabongo, Ivan. Macia, Oscar E. Ruiz, and Julian. Florez. (2015), “Ultrasound Image Dataset for Image Analysis Algorithms Evaluation.” in *Innovation in Medicine and Healthcare*, vol 45: 447–457.
- [18] Islam. Aly, Asad. Rizvi, Wallisa. Roberts, Shehzad. Khalid, Kassem, Sonja. Salandy, Maira, R. Shane Tubbs, Marios. Loukas. (2021), “Cardiac ultrasound: An Anatomical and Clinical Review.” *Translational Research in Anatomy*, vol. 22, p. 100083.
- [19] Dorland. (2011), “Dorland’s Illustrated Medical Dictionary.” Elsevier Health Sciences, p1461.
- [20] U. F. O. Themes. (2019), “Cardiac Ultrasound Technique.” *Radiology Key*. [Online]. Available: <https://radiologykey.com/cardiac-ultrasound-technique/>.
- [21] Ahmed. Intisar and Sasikumar. Navaneetha. (2023), “Echocardiography Imaging Techniques.” in *StatPearls*, Treasure Island (FL): StatPearls Publishing, [Online]. Available: <http://www.ncbi.nlm.nih.gov/books/NBK572130/>.
- [22] ‘Parasternal Long Axis’, *Echocardiographer*. Or. [Online]. Available: <https://www.echocardiographer.org/tte-plax>.
- [23] John Edward. Hall and Arthur C. Guyton. (2011), *Guyton and Hall Textbook of Medical Physiology*. Saunders/Elsevier, pp. 105-107.
- [24] The Editors of Encyclopaedia Britannica. (1998), “Systole | Definition, Cycle, & Facts | Britannica”. [Online]. Available: <https://www.britannica.com/science/systole-heart-function>.